JOURNAL OF APPLIED ELECTROCHEMISTRY **26** (1996) 51–57

# Electrochemical behaviour of silver-containing copper anodes under simulated electrorefining conditions

E. A. KUCHARSKA-GIZIEWICZ, D. J. MACKINNON

*Minerals Sciences Laboratories, CANMET, Department of Natural Resources Canada, 555 Booth Street, Ottawa, Ontario, Canada K1A 0G1*

Received 17 January 1995; revised 24 April 1995

Cyclic voltammetry was used to characterize the behaviour of silver-bearing copper anodes during electrorefining. Reproducible electrochemical characteristics were obtained for copper anodes of different shapes, sizes and configurations (vertical against horizontal) containing up to 1 wt % silver. Passivation time measurements indicated a strong correlation between the electrochemical spectra characteristics and the ease of anode passivation. A cubic-shaped anode without acrylic mounting medium was developed that avoided the impact of anode size and shape on the electrochemical characteristics and passivation of silver-bearing copper anodes. A fully computerized data acquisition system previously developed to generate electrochemical spectra for pure copper anodes under simulated electrorefining conditions has been extended to the examination of silver-bearing copper anodes.

## 1. Introduction

The behaviour of silver contained in the anodes subjected to copper electrorefining has been the topic of several investigations. Basic studies [1–9] have established that for silver concentrations up to approximately 1%, the silver contained in copper anodes exists mostly in solid solution. The Ag-bearing copper crystals have a potential which is approximately 30 mV more noble than that of pure copper but still much lower than that of pure silver. During electrorefining, silver and copper dissolve together with the dissolved silver is reprecipitated by a number of complex reactions. In sulphate media containing elemental copper and its univalent ions, silver is deposited as a relatively compact layer on the anode surface. Part of the silver, however, remains in solution and is possibly deposited with the copper at the cathode. According to Noguchi *et al.* [10], silver forms a very adhesive layer that accelerates passivation of the anode.

Chen and Dutrizac [11] carried out a detailed mineralogical study of various copper anodes and copper refinery anode slimes to elucidate the behaviour of silver during copper electrorefining. During electrorefining, part of the dissolved silver precipitates as metallic silver. The morphology of the silver particles indicates a dissolution–precipitation mechanism. Some metallic silver may form by cementation on the copper surface:

$$Ag^+ + Cu \longrightarrow Ag + Cu^+ \qquad (1)$$

To account for the observed precipitation of metallic silver on $Cu_2O$, selenides or $CuSO_4 \cdot 5H_2O$, it was proposed that part of the dissolved silver also reacts with cuprous ions according to:

$$Cu^+ + Ag^+ \longrightarrow Ag + Cu^{2+} \qquad (2)$$

During the electrorefining of commercial anodes, however, much of the silver reacts with the $Cu_2(Se, Te)$ inclusions liberated from the anode to form sequentially, silver-bearing copper selenide, AgCuSe, copper-bearing silver selenide and $Ag_2Se$ according to the reactions:

$$Cu_2Se + x\,Ag^+ \longrightarrow (Cu_{2-x}Ag_x)Se + x\,Cu^+ \qquad (3)$$

$$(Cu_{2-x}Ag_x)Se + (1-x)Ag^+ \longrightarrow AgCuSe + (1-x)Cu^+ \qquad (4)$$

$$AgCuSe + (1-x)Ag^+ \longrightarrow Ag_{2-x}Cu_x + (1-x)Cu^+ \qquad (5)$$

$$(Ag_{2-x}Cu_x)Se + x\,Ag^+ \longrightarrow Ag_2Se + x\,Cu^+ \qquad (6)$$

All the selenide species are tellurium-bearing. The reactions begin at the surface of the corroding copper anode and continue into the slimes attached to the anode surface and finally into the slimes resting on the bottom of the refining cells. Although the reactions are rapid, equilibrium is not fully attained and thus many silver-bearing species are present in the anode slimes.

Kuxmann and Meyer [12] observed that during the electrorefining of copper anodes containing silver as the only impurity, passivation was accompanied by an increased oscillating voltage that resulted in an increase in the silver content of both the electrolyte and cathode. At a current density of $230\,A\,m^{-2}$, with anodes containing $< 0.25\%$ Ag, the cell voltage was in the 100–130 mV range and rose slightly over the 92 h electrolysis period. For anodes containing $> 0.25\%$ Ag, the cell voltage oscillated, with peak values of 1–2 V at different frequencies and amplitudes, about a mean of approximately 200 mV over the 92 h period. The oscillations were a result of passivation phenomena. When the current density was doubled, the start of oscillations shifted to lower anode silver contents. The cell voltage started oscillating earlier with increasing anode silver contents. Oscillations begin when the adhering slimes layer reaches a critical thickness and anode passivation with greatly increased voltage peaks occurs. At the same time, the dissolution potential of pure silver is reached so that ionic silver dissolves into the electrolyte and some subsequently deposits at the cathode.

A computerized data acquisition method based on cyclic voltammetry that gave reproducible results for the electrochemical behaviour of pure copper anodes under simulated electrorefining conditions was described in a previous paper [13]. The method allows the data to be presented as a potential–current–time spectrum, that is, an electrochemical spectrum, rather than as a conventional cyclic voltammogram. The electrochemical spectrum format greatly enhances the clarity and readability of the experimental results.

The results of the previous study [13] confirmed that the formation of a second current density peak on the electrochemical spectrum was associated with the anode slimes that remained attached to the surface. In the present study, the technique has been applied to silver-containing copper anodes to determine the effect of silver on second peak formation and its relationship to the tendency of the anode to passivate. The results are interpreted on the basis of those obtained previously for pure copper anodes under similar conditions.

## 2. Experimental details

Copper rods measuring 20 cm long by 5 cm in diameter and containing various amounts of silver were prepared for Canmet by the Noranda Technology Centre. Anodes were prepared by cutting rectangular sections from the cast rods. Two different anode fabrication designs were used: acrylic mount and hanging piece. The copper anodes, mounted in acrylic, had only a single face exposed to the electrolyte. Electrical contact was achieved by drilling through the back of the acrylic mount into the copper. A brass rod was threaded into the copper and this served as the external electrical contact. The brass rod was insulated from the electrolyte by a tight-fitting sleeve of Tygon® tubing which was sealed into the acrylic mount with silicone rubber. Some of the acrylic-mounted electrodes were also positioned horizontally in the electrochemical cell such that the slimes produced during electrorefining stayed on the surface of the anode. Larger anodes were prepared by threading a brass rod, contained in a tight-fitting sleeve of Tygon® tubing, into the top of the sample and sealing it with silicone rubber. At the same time, the top and back edge of the sample were also insulated. Thus, in this design, four edges of the cubic-shaped anode were in contact with the solution.

Cyclic voltammetry (CV) studies were performed using a conventional water-jacketed cell with a copper working electrode, a platinum counter electrode and a mercury/mercurous sulphate reference electrode. A Luggin capillary, the tip of which was set at a distance of 1 cm from the surface of the working electrode, was used to minimize uncompensated resistance effects. A PAR 173 potentiostat/galvanostat equipped with plug-in module M376, was used as a potentiostat allowing the anode to be maintained at various programmed potentials with respect to the reference electrode. A Hokuto Denko HA-310 10 A potentiostat/galvanostat was used to examine the larger anodes. A PAR 175 universal programmer provided various potentiodynamic voltage vs time programs. The $I/V$ profiles were recorded via an analog to digital Keithly MetraByte DAS-16 board. The DAS-16 board was installed directly into a computer expansion slot, thereby turning the computer into a high precision data acquisition instrument.

The CV experiments were conducted in aqueous solutions containing $40\,\mathrm{g\,dm^{-3}}$ $Cu^{2+}$ as $CuSO_4$ and $160\,\mathrm{g\,dm^{-3}}$ $H_2SO_4$ at 65°C as these conditions approximate those used in commercial electrorefining operations. The cell electrolyte was heated and maintained at the desired temperature using a circulation water bath. Experiments were performed in an air atmosphere and the electrolyte was not stirred. The surfaces of the copper anodes were prepared by grinding on a diamond wheel (45 $\mu$m). Just before an experiment, a quick grind at 100 $\mu$m was done, followed by a rinse with doubly distilled water. Polishing was not done, as it was discovered that polishing gave less reproducible results; this effect is attributed to the initial 'attack' required to dissolve the polished surface.

The Ag-bearing copper anodes were subjected to a controlled number of continuous potential cycles ranging between −0.35 V and 0.0 V in the initial experiments and between −0.35 and +0.4 V in the subsequent experiments, at a scan speed of $2\,\mathrm{mV\,s^{-1}}$. The scan speed of $2\,\mathrm{mV\,s^{-1}}$ was chosen after establishing that the potentials at which the peaks form are scan speed dependent. This speed seemed low enough to accommodate second peak formation without unduly lengthening the experiment. Initial measurements concentrated on smaller size anodes $<1\,\mathrm{cm^2}$. The potential range of −0.35 to 0.0 V was chosen because of the distinct differences in the electrochemical behaviour displayed by anodes with various impurity contents in this potential region. The anodes were always disconnected at the 'cathodic end' of the sweep (at −0.35 V), and usually after 30 cycles. It was observed, however, that the second peak formation was not only a product of the impurity content of the anodes but was also dependent on the cavity formed during the experiment between the wall of acrylic and the dissolving copper sample. This cavity helped to retain the slimes on the surface. Measurements using larger anodes showed that as the ratio of the surface area to cavity area increases the behaviour of the anodes in this potential range changes and the second peak no longer forms regardless of the anode impurity content. The idea of using a broader potential range for the larger anodes was introduced as a means of duplicating the previously acquired results. In examining the larger electrodes (> 4 cm$^2$), sampling of four points per second was used and usually 20 cycles were acquired.

In other experiments, passivation times were determined for selected anodes by maintaining the anodes at constant current and monitoring the potential–time profiles. A PAR 362 potentiostat/galvanostat was used as a galvanostat allowing the anode to be maintained at a constant current. The onset of passivation was signalled by an abrupt increase in the anode potential. The time required for this potential increase to occur is denoted at $t_p$, time to passivation. The $t_p$ values were determined using the same cell and electrolyte composition as for the CV experiments. A constant current, equivalent to 900 A m$^{-2}$ current density, and a temperature of 45°C were chosen to ensure that the silver-containing anodes would passivate in a reasonable time period. Commercial copper electrorefining is normally carried out at a current density of 250 A m$^{-2}$ and a temperature of 65°C.

## 3. Results and discussion

### 3.1. *Effect of silver*

The typical electrochemical behaviour for copper anodes of 0.9 cm$^2$ surface area, mounted in acrylic and configured vertically in the electrochemical cell, is shown in Figs 1 and 2. The potential profile imposed on the anode is represented by the dashed line, whereas the solid line represents the current response to the applied potential. The electrochemical spectrum obtained for pure copper, Fig. 1, indicates that current oscillations develop during the 3rd cycle and remain fairly consistent through the 30th cycle. For the 0.5% Ag–Cu anode, Fig. 2, strong oscillations occur during the second cycle and a current density minimum or second peak occurs on the seventh cycle. This second peak grows and the oscillations gradually diminish as the potential scan is continued through 30 cycles. The second peak, Fig. 2, is associated with a slimes layer of Ag powder and copper sulphate that adheres to the anode surface. Although Cu powder forms during the dissolution of pure copper anodes, it does not adhere to the surface and hence the second peak does not appear [13].

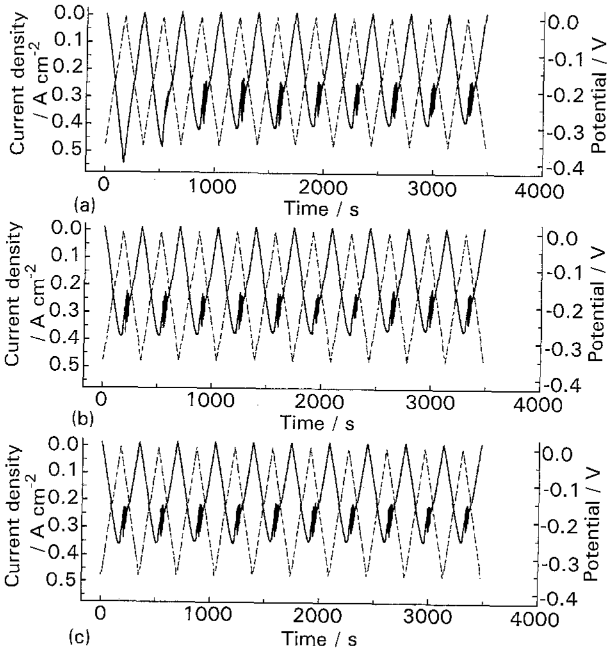

Fig. 1. Electrochemical spectra of thirty continuous cycles (cycle 1 to cycle 30) recorded for a 0.9 cm$^2$ rectangular pure copper anode configured vertically. (a) Cycles 1–10, (b) cycles 11–20, (c) cycles 21–30. The potential profile is given by the dashed line and the current response corresponds to the solid line.

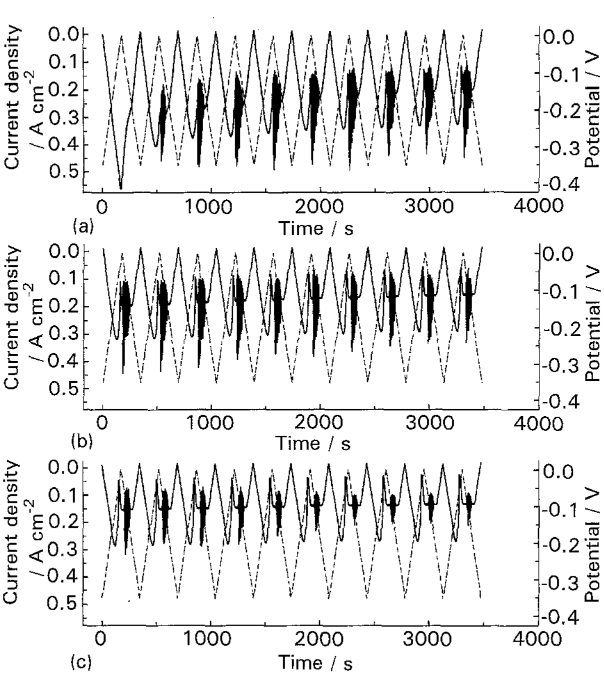

Fig. 2. Electrochemical spectra of thirty continuous cycles recorded for a 0.9 cm$^2$ rectangular 0.5% Ag–Cu anode configured vertically. (a) Cycles 1–10, (b) cycles 11–20, (c) cycles 21–30.

The effect of the silver content of the copper anode on the electrochemical spectrum is shown in Fig. 3. The spectra shown were obtained for 0.6 cm$^2$ anodes mounted in acrylic. For the 0.1% Ag–Cu anode, Fig. 3(a), oscillations begin from the first cycle and increase in intensity with continued cycling. The second peak becomes noticeable by about the 5th or 6th cycle appearing as it emerges from behind the oscillations. The 0.5% Ag–Cu anode, Fig. 3(b), is characterized by intense oscillations on the 1st cycle with the second peak emerging by the 3rd cycle. As cycling continues, the second peak grows and the oscillations diminish in intensity. The second peak is larger and occurs at a less anodic potential than that for the 0.1% Ag–Cu anode. For the 1% Ag–Cu anode, Fig. 3(c), the second peak is already well established and the intense oscillations have virtually disappeared by the 2nd cycle. The second peak occurs at the same potential as that for the 0.5% Ag–Cu anode. The occurrence of current oscillations is an indication of the disintegration or spalling of a weakly

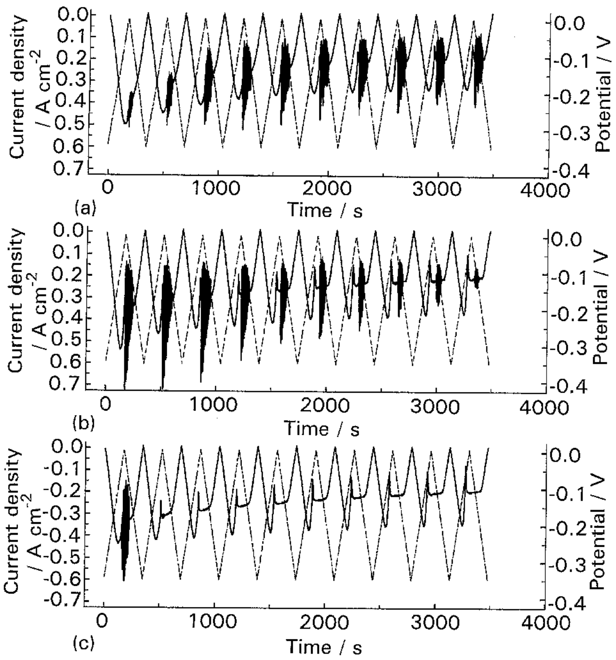

Fig. 3. Electrochemical spectra of ten continuous cycles (cycles 1 to 10) recorded for the 0.6 cm$^2$ rectangular copper anodes containing (a) 0.1% Ag, (b) 0.5% Ag, (c) 1% Ag, configured vertically.

adherent, porous surface layer. The formation of the second peak and diminished intensity of the current oscillations with increasing anode Ag content indicate that the surface layer becomes more adherent and less porous as the Ag content increases. As shown in a previous study [13], the tendency for the anode to retain the slimes layer and thus form the second peak makes it more prone to passivation.

The surfaces of the silver-containing copper anodes were examined by SEM/EDX after 30 cycles of potential. The results obtained for a 1% Ag–Cu anode are shown in the series of SE micrographs, Fig. 4. The slimes layer shown in Fig. 4(a) consists of silver powder and copper sulphate. Fig. 4(b) shows the structure of the copper sulphate crystals, some of which have attached silver powder. Fig. 4(c) shows the silver powder in more detail. The fact that Ag powder forms on the copper sulphate crystals is indicative of Ag dissolution followed by the reaction of $Ag^+$ with $Cu^+$, Equation 2.

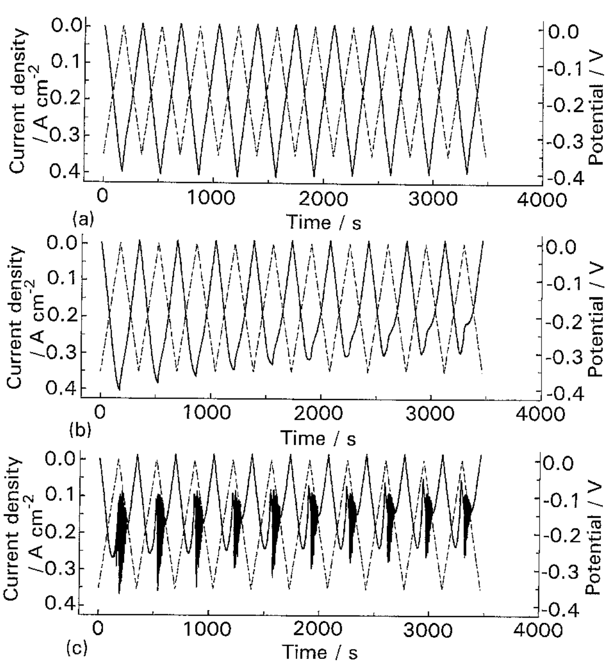

Fig. 5. Electrochemical spectra of ten continuous cycles (cycles 1 to 10) recorded for a rectangular pure copper anode, area 2.1 cm$^2$ (a) and 0.5% Ag-copper anodes (area 1.5 cm$^2$) configured vertically (b) and horizontally (c).

### 3.2. *Effect of anode size and configuration*

In a previous study [13], it was found that the electrochemical behaviour of pure copper anodes was affected by their size and shape that influenced the dissolution pattern and hence the tendency for the anode to retain the slimes layer. This behaviour also was observed for the Ag-containing anodes used in the present study as indicated by comparing Figs 2(a) and 3(b). For the smaller anode, Fig. 3(b), the oscillations and second peak formation occur earlier than they do for the larger anode, Fig. 2(a). Fig. 5(a) shows the electrochemical spectra obtained for a pure copper anode (area = 2.09 cm$^2$). Fig. 5(b) and (c) illustrate the spectra realized for a 0.5% Ag-copper anode of similar size. In the case of pure copper configured vertically and cycled in the potential range between −0.35 and 0.0 V vs MSE, Fig. 5(a), Cu powder forms but unlike the smaller anode (Fig. 1), it is not retained

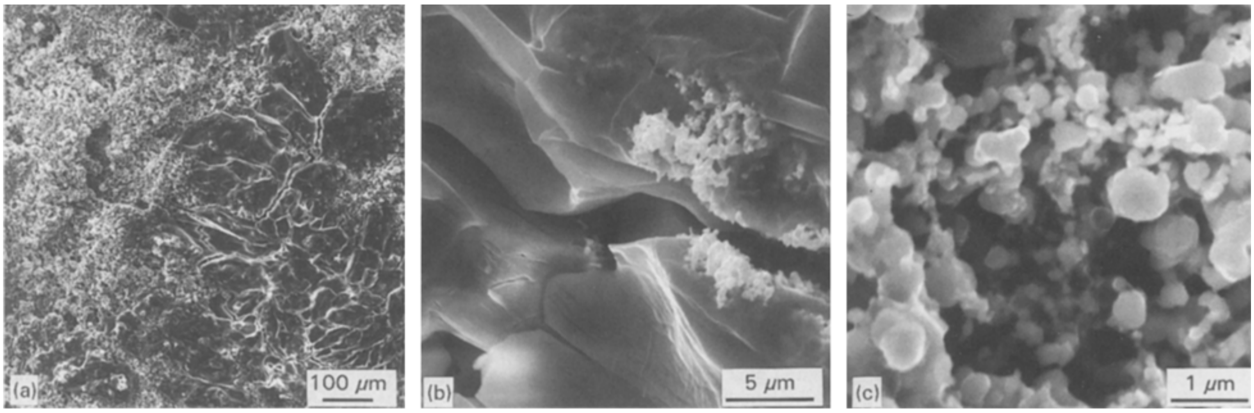

Fig. 4. Secondary electron micrograph showing the morphology of the slimes layer formed on a 1% Ag–Cu anode after 30 cycles. (a) General view, (b) copper sulphate structure, (c) silver powder detail.

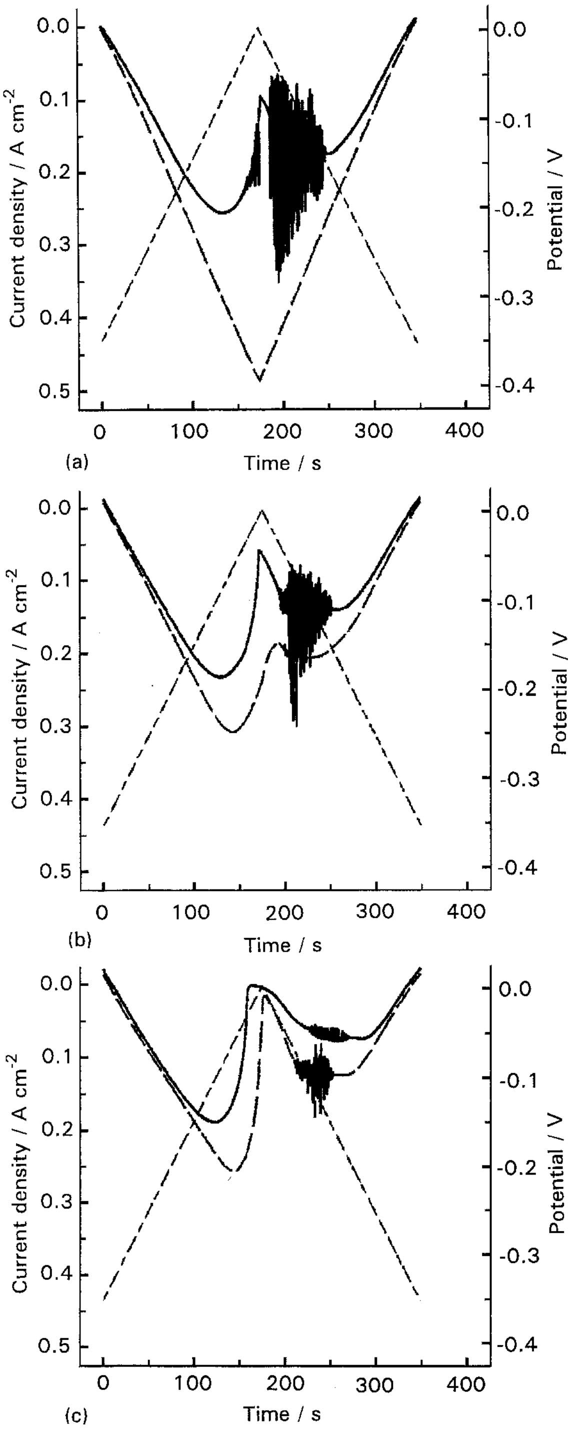

Fig. 6. Electrochemical spectra of the first (a), 10th (b) and 60th (c) cycles recorded for a 0.5% Ag–Cu anode configured vertically (dashed line) and horizontally (solid line).

on the surface. Thus, copper dissolution is essentially ideal, and no current oscillations or second peak formation was observed. For the 0.5% Ag–Cu anode configured vertically, Fig. 5(b), a small shoulder associated with an Ag, Cu, $CuSO_4 \cdot xH_2O$ slimes layer becomes noticeable by about the 5th cycle. This is in contrast to the smaller anode, Fig. 2(b), where intense oscillations occur on the 1st cycle and the second peak is noticeable by the 3rd cycle. Thus, the smaller anodes have a greater tendency to retain the slimes layer due to the cavity formed in the acrylic mount as the copper anode dissolves.

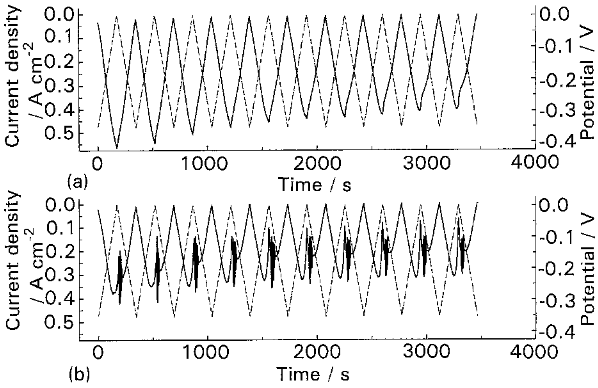

Fig. 7. Electrochemical spectra of ten continuous cycles (cycles 1 to 10) recorded for a 0.5% Ag–Cu anode configured (a) vertically and (b) horizontally in a cell containing $H_2SO_4$ electrolyte.

The effect of the slimes layer on the current oscillations and second peak formation was confirmed by comparing the electrochemical spectra for the 0.5% Ag–Cu anode configured vertically, Fig. 5(b), and horizontally, Fig. 5(c), within the cell. As mentioned above, current oscillations are not observed for the vertically configured anode, but a shoulder begins to form during the 4th cycle and becomes more defined with continuous cycling. This is indicative of some slimes retention on the vertical surface. The horizontally configured electrode, however, clearly displays intense current oscillations. Second peak formation occurs on the 2nd cycle, as the slimes are retained on the horizontal anode surface. The second peak is enhanced with continuous cycling as the slimes accumulate on the anode surface and trap more nonconductive solid copper sulphate. As cycling continues, there is a considerable difference in the thickness and adherence of the slimes layers as a result of the different configurations. The horizontally configured anode possesses a thicker and more adhered slimes layer than manifests itself on the electrochemical spectra with fewer oscillations and a broader second peak. These features are clearly seen in the comparison between the electrochemical spectra of the first, 10th and 60th cycles of the same 0.5% Ag–Cu anode configured vertically and horizontally as presented in Fig. 6.

To examine the effect of copper ion concentration on the electrochemical behaviour of silver-containing copper anodes, an experiment was carried out in a solution containing only $H_2SO_4$. The results obtained for a 0.5% Ag–Cu anode configured vertically and horizontally in the cell are presented in Fig. 7. The electrochemical spectra are similar to those realized in the presence of $Cu^{2+}$, Fig. 5, but with subtle differences. For the vertically configured anode, cf. Figs 5(b) and 7(a), the maximum current density is much higher and the shoulder forms more slowly in the absence of $Cu^{2+}$ ions. Similarly, for the horizontally placed anode, cf. Figs 5(c) and 7(b), the oscillations are less intense and the second peak is more slowly developed in the absence of $Cu^{2+}$ ions. These differences may be attributed to the fact that in the $H_2SO_4$ solution, the diffusion of $Cu^{2+}$ ions into

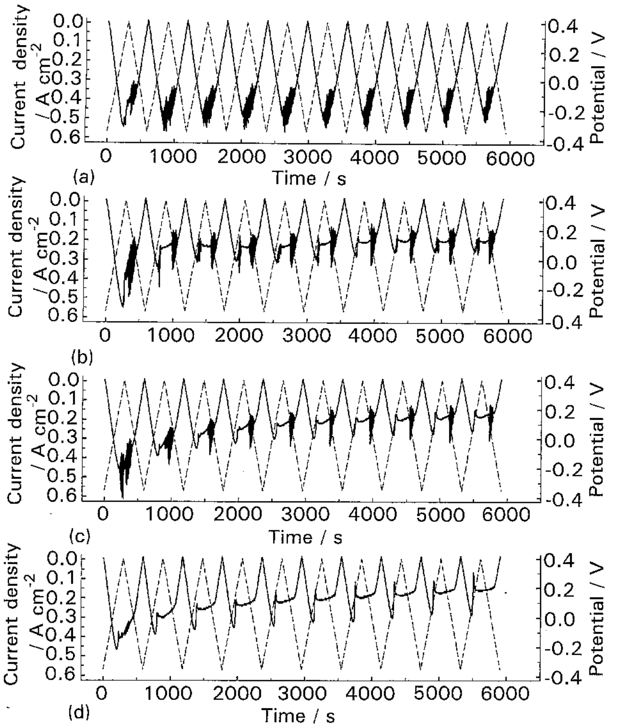

Fig. 8. Electrochemical spectra of ten continuous cycles (cycles 1 to 10) recorded for large, cube-shaped pure copper (a), 0.1% Ag–Cu (b), 0.5% Ag–Cu (c) and 1% Ag–Cu (d) anodes.

solution was not initially inhibited by a high concentration of $Cu^{2+}$ ions in the vicinity of the anode.

### 3.3. *Large anodes*

The electrochemical characteristics of the larger pure copper and silver-bearing copper anodes ($>4\,cm^2$) were also determined. As described in Section 2, these anodes were cube-shaped and were not mounted in acrylic; they had four faces exposed to the electrolyte. Thus, they more closely simulated industrial practice, and also, any effect of the acrylic mounting medium on slimes retention was eliminated. It was hoped that this anode design would eliminate the anode "size" effect on the electrochemical characteristics. For the experiments involving these large anodes, it was necessary to extend the potential range from 0.0 to +0.4 V vs MSE to reproduce the electrochemical characteristics obtained using the smaller, acrylic-mounted anodes.

In Fig. 8, the electrochemical spectra obtained for large, cube-shaped, pure copper, 0.1% Ag–Cu, 0.5% Ag–Cu and 1% Ag–Cu anodes are compared. The electrochemical spectrum from the pure copper anode, Fig. 8(a), has no second peak but displays intense current oscillations which is related to the spalling of the copper powder which forms but is not retained on the surface. The maximum current density for copper dissolution is higher for this anode than for the other anodes presented in the Figure.

For the 0.1% Ag–Cu anode, the electrochemical spectrum, Fig. 8(b), features current oscillations but the retention of the slimes on the anode surface is strong enough to form a second peak. Although a peak forms by the 7th cycle, it diminishes in the 9th cycle as spalling characterized by oscillations takes place. For anodes containing 0.5% Ag, Fig. 8(c), the current oscillations remain and the second peak develops by the 6th cycle. Finally at 1% Ag, Fig. 8(d), the electrochemical spectrum is characterized by a sharply defined second peak with no current oscillations. This indicates a strongly adsorbed, nonporous slimes layer and hence a greater tendency for the anode to passivate.

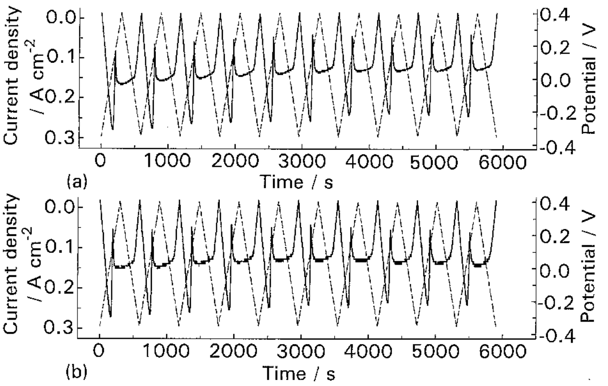

Fig. 9. Electrochemical spectra of ten continuous cycles (cycles 11 to 20) recorded for two large 1% Ag–Cu anodes, (a) $4.045\,cm^2$ and (b) $7.885\,cm^2$.

Increasing the size of the anode by a factor of ~2 resulted in very similar electrochemical spectra as shown in Fig. 9. The 11th–20th cycles for 1% Ag–Cu anodes, Fig. 9(a), $4.045\,cm^2$ and Fig. 9(b), $7.885\,cm^2$, are practically identical. Hence, the anode size factor seems to have been eliminated.

### 3.4. *Passivation*

It was shown previously [13] that a direct correlation existed between second peak formation and passivation time. In the present study it was shown that an increasing silver content in the copper anode facilitates second peak formation and also promotes passivation. The results obtained for passivation time measurements on vertically configured copper anodes ($<1\,cm^2$) containing various silver concentrations are shown as a plot of passivation time, $t_p$, against Ag concentration in the anode, Fig. 10. As indicated, the passivation time decreases with increasing Ag content in the copper anode. Initially, the

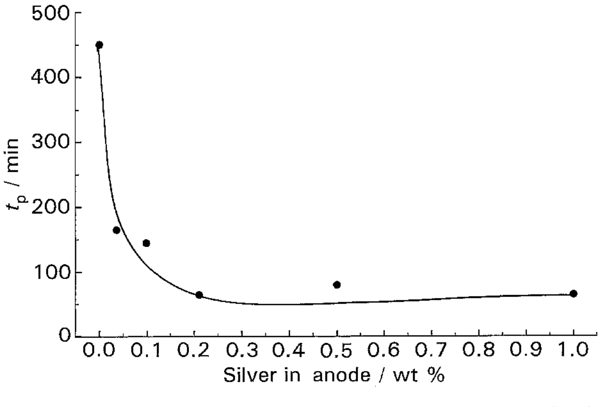

Fig. 10. Plot of passivation time, $t_p$, against silver concentration in the anode.

decrease in passivation time is very rapid for Ag contents to 0.2 wt %; for Ag concentrations between 0.2 and 1 wt %, $t_p$ remained constant at approximately 65 min under the experimental conditions used.

Just as increasing size of the Ag–Cu anodes delayed second peak formation in the CV experiments, it also resulted in an increase in the passivation time. For example, increasing the area of the 1% Ag–Cu anode from roughly 1 to 2.3 $cm^2$ increased the passivation time from 65 to 125 min; i.e., it reduced the tendency of the anode to passivate. This tendency, as noted previously for pure copper anodes [13], is related to the ability of the smaller acrylic-mounted anodes to retain the slimes layer.

Some of the large, silver-containing copper anodes, not mounted in acrylic, were also subjected to passivation measurements to determine $t_p$. The 0.5% and 1% Ag–Cu anodes which formed a well defined second peak (Fig. 9) gave $t_p$ values of 110 min and 92 min, respectively.

## 4. Conclusion

The electrochemical behaviour of silver-containing copper anodes under simulated electrorefining conditions was determined. The electrochemical spectra were characterized by current oscillations and the formation of a second peak. The intensity of the current oscillations and ease of formation of the second peak were dependent on the silver content of the anode, the anode configuration in the cell, and the anode fabrication mode. At high silver contents ($\geqslant 0.5\%$ Ag) a stable, adherent slimes layer consisting of Ag and copper sulphate formed on the anode surface and resulted in a well-formed second peak on the electrochemical spectrum. The second peak formed more readily when the anodes were configured horizontally within the cell as slimes retention was aided by gravity. For anodes mounted in acrylic, the actual size of the anode was important as the cavity formed due to copper dissolution aided slimes retention. The effect of anode size on the electrochemical spectra was overcome by eliminating the acrylic mount. Large ($>4\,cm^2$), cube-shaped anodes with four edges exposed to the electrolyte gave reproducible, characteristic electrochemical spectra, when the potential was scanned between $-0.35$ and $+0.4$ V against MSE at a scan speed of $2\,mV\,s^{-1}$. Passivation time measurements confirmed a strong correlation between the above electrochemical behaviour of the silver-bearing copper anodes and their tendency to passivate.

## Acknowledgements

Thanks are due to J. E. Dutrizac, CANMET, for many helpful discussions and to the Noranda Technology Centre for preparing some of the anode material.

## References

[1] P. Graumann, C. Fisher-Bartelk and D. Schab *N. Hütte* **17** (1972) 71–6.

[2] U. Kuxmann and H. Weber, *Metall* **27** (1973) 19–27.

[3] U. Schulz, K. Hein and D. Schab *N. Hütte* **21** (1976) 261–5.

[4] H.-J. Lange, K. Hein and D. Schab, *Freib. Forsch.-H.* **B195** (1977) 29–49.

[5] H.-J. Lange, K. Hein, D. Schab and B. Geidel, *Erzmetall* **30** (1977) 369–74.

[6] J. Sedzimir, *Arch. Hutnictwa* **21** (1976) 31–43.

[7] *Idem, ibid.* **29** (1984) 195–214.

[8] V. Baltazar, P. L. Claessens, J. Thiriar and J. Lapierre, *in* 'Extraction Metallurgy '89'. The Institute of Mining and Metallurgy, London (1989) 939–51.

[9] V. Baltazar and J. Caissey, *in* 'Copper '91' (edited by W. C. Cooper, D. J. Kemp, G. E. Lagos and K. G. Tan), Vol. III, Pergamon, New York (1991) pp. 329–40.

[10] F. Noguchi, Y. Iida, T. Nakamura and Y. Ueda, *Shigem to Sozai* **107**(8) (1991) 569–75.

[11] T. T. Chen and J. E. Dutrizac, *Metall Trans* **20B** (1989) 345–61.

[12] U. Kuxmann and U. Meyer, *Erzmetall* **46** (1993) 346–55.

[13] E. A. Kucharska-Giziewicz and D. J. MacKinnon, *J. Appl. Electrochem.* **24** (1994) 953–64.